AIP The Journal of Chemical Physics

Application of the quasi-variational coupled cluster method to the nonlinear optical properties of model hydrogen systems

James B. Robinson and Peter J. Knowles

Citation: J. Chem. Phys. **137**, 054301 (2012); doi: 10.1063/1.4738758
View online: http://dx.doi.org/10.1063/1.4738758
View Table of Contents: http://jcp.aip.org/resource/1/JCPSA6/v137/i5
Published by the American Institute of Physics.

THE JOURNAL OF CHEMICAL PHYSICS **137**, 054301 (2012)

Application of the quasi-variational coupled cluster method to the nonlinear optical properties of model hydrogen systems

James B. Robinson and Peter J. Knowles[a)]
School of Chemistry, Cardiff University, Main Building, Park Place, Cardiff CF10 3AT, United Kingdom

(Received 24 April 2012; accepted 8 July 2012; published online 1 August 2012)

We present a pilot application of the recently proposed quasi-variational coupled cluster method to the energies, polarizabilities, and second hyperpolarizabilities of model hydrogen chains. Relative to other single-reference methods of equivalent computational complexity, we demonstrate this method to be highly robust and especially useful when traditional coupled cluster theory fails to perform adequately. In particular, our results indicate it to be a suitable method for the black-box treatment of multiradicals, making it of widespread general interest and applicability. © *2012 American Institute of Physics*. [http://dx.doi.org/10.1063/1.4738758]

I. INTRODUCTION

The nonlinear optical (NLO) properties of a molecule are responsible for macroscopic phenomena such as refractive indices,[1] and the design of materials exhibiting large or systematically tunable NLO properties is of great interest for use in both current and future generations of optoelectronic devices.[2–7] Owing to this interest, a great deal of experimental[8–12] and theoretical[10–14] work has been targeted at this area. Linearly conjugated organic polymer chains have been extensively studied due to the discovery of relationships between structural and NLO properties,[15–22] and, for singlet multiradicals in particular, studies on models have found the second hyperpolarizability to depend strongly on the diradical character.[23,24] This has been confirmed theoretically for systems such as graphene nanoflakes,[25,26] as well as experimentally.[27,28]

The first investigation of molecular NLO properties using highly correlated wavefunction methods was performed by Bartlett and Purvis,[29] and a correct treatment of electron correlation has since been shown to be essential in obtaining quantitatively accurate values of NLO properties from theoretical methods,[30–38] especially second hyperpolarizabilities, which Hartree-Fock[39,40] (HF) theory is known to systematically underestimate. Unfortunately, the common variants of density functional theory[41,42] overestimate these same NLO properties,[43,44] and while more novel approaches have lessened this problem, it has yet to be fully resolved.[45,46]

Due to the size and complexity of many of the systems of interest, *ab initio* calculations are typically applied to smaller representative test cases[24] or else resort to the investigation of model hydrogen chains as prototypical multiradicals[23,47–52] in order to benchmark other, less expensive methods.[31,36,53,54] However, since the NLO properties are extremely sensitive to the treatment of electron correlation,[30,55,56] it has also become important to benchmark the *ab initio* methods amongst themselves on these systems.[32,37] For this purpose, it has become common to use traditional coupled cluster[57–62] (TCC) limited to single and double excitations of the HF reference determinant (CCSD) in order to achieve a highly correlated approximation to the many-body Schrödinger wavefunction, sometimes combined with a correction to the calculated energy motivated by perturbative estimates of the effect of triple excitations.[63–65]

Unfortunately, TCC itself performs poorly when the Hartree-Fock approximation on which it is based becomes qualitatively wrong and a single-determinantal reference wavefunction becomes a poor model of the exact electronic wavefunction. This is especially problematic for multiradicals and geometries far from equilibrium, which are often the systems of interest in the context of applications to nonlinear optics.[24] If the TCC energy becomes poor as a result of this problem, the effect will be magnified for higher order properties, such as second hyperpolarizabilities. Furthermore, the multireference methods, such as multireference configuration interaction[66,67] and related formulations that seek to approximately correct for size-extensivity errors,[68–70] while more reliable in such situations, do not operate in a "black-box" fashion, and are thus more difficult to deploy on large systems. They also often suffer from unfavourable computational scaling and problems stemming from the lack of rigorous extensivity.

We have recently put forward a new single-reference post-Hartree-Fock method, quasi-variational coupled cluster[71] (QVCC), that deals more effectively with nondynamic correlation at the doubles level (QVCCD). This is the most advanced of a family of methods[72,73] that function by constructing an infinite-order approximation to VCC (Ref. 74) restricted to double excitations (VCCD), which has been demonstrated previously by several other authors[75–81] to be significantly more robust than TCC, due to the stabilizing property that calculated VCC energies are upper bounds on the exact ground-state Schrödinger energy eigenvalue. In fact, poor performance of CCSD can be directly attributed to its divergence from VCCSD,[82] and modifications of CCSD have been devised to correct for this.[83–85] Unfortunately, the computational complexity of these corrections exceeds that of the limiting step of a CCSD calculation, so they have

---

[a)] Electronic mail: KnowlesPJ@Cardiff.ac.uk.

not been widely adopted. In contrast, the limiting step of a quasi-variational coupled cluster calculation is identical with that of CCSD. When combined with orbital optimization[86] to deal with single excitations, as well as a standard perturbative triples correction[63] to capture remaining dynamic correlation effects, the resulting OQVCCD(T) method is capable of predicting both a physically correct and quantitatively accurate potential energy curve for the dissociation of dinitrogen, N_2,[87] and other strongly correlated molecules.[88] In this article, we investigate whether the quasi-variational coupled cluster method also provides a more robust description of the electron correlation of multiradicals and their NLO properties by investigating the singlet states of several model hydrogen systems.

II. THEORY

Using the Einstein summation convention[89] and a spin-orbital notation in which the sets $\{i, j, k, \dots\}$ and $\{a, b, c, \dots\}$ denote orbitals occupied and unoccupied in the single-determinantal reference wavefunction, $|\Phi_0\rangle$, respectively, the QVCCD (Ref. 71) ground-state energy is the minimum of the following functional with respect to the set, $\{T_{ab}^{ij}\}$, of doubles-only cluster amplitudes:

$$E = \langle\Phi_0|\hat{H}(1 + 2\,{}_2\hat{T})|\Phi_0\rangle + \langle\Phi_0|\,{}_1\hat{T}^\dagger\,\hat{H}_1\hat{T}|\Phi_0\rangle_L. \tag{1}$$

The ${}_q\hat{T}$ operators are defined as follows:

$${}_q\hat{T}|\Phi_0\rangle = \tfrac{1}{4}\,{}_qT_{ab}^{ij}\,\big|\Phi_{ij}^{ab}\big\rangle, \tag{2}$$

$$\begin{aligned}{}_qT_{ab}^{ij} &= (1-\tau_{ab})({}_{\mathcal{A}}\mathbf{U}^{-\frac{q}{2}})_a^c T_{cb}^{ij}\\ &\quad + (1-\tau_{ij})({}_{\mathcal{B}}\mathbf{U}^{-\frac{q}{2}})_k^i T_{ab}^{kj}\\ &\quad - \tfrac{1}{2}({}_{\mathcal{C}}\mathbf{U}^{-\frac{q}{2}})_{kl}^{ij} T_{ab}^{kl}\\ &\quad - \tfrac{1}{2}(1-\tau_{ij})(1-\tau_{ab})({}_{\mathcal{D}}\mathbf{U}^{-\frac{q}{2}})_{ak}^{ic} T_{cb}^{kj},\end{aligned} \tag{3}$$

$$\begin{aligned}{}_{\mathcal{A}}U_b^a &= \delta_b^a + \tfrac{1}{2}T_{bc}^{ij}\,T_{ij}^{ac} \qquad & {}_{\mathcal{C}}U_{kl}^{ij} &= \delta_{kl}^{ij} + \tfrac{1}{2}T_{ab}^{ij}\,T_{kl}^{ab},\\ {}_{\mathcal{B}}U_j^i &= \delta_j^i + \tfrac{1}{2}T_{ab}^{ik}\,T_{jk}^{ab} \qquad & {}_{\mathcal{D}}U_{aj}^{ib} &= \delta_{aj}^{ib} + T_{ac}^{ik}\,T_{jk}^{bc},\end{aligned} \tag{4}$$

where the operator τ_{pq} permutes the labels p, q in what follows, and the L subscript denotes the inclusion of fully linked terms only. Single excitations may be incorporated into this scheme by minimization of the functional also with respect to the orbitals (OQVCCD),[86] or by the use of the Brueckner constraint (BQVCCD).[90–92] Our functional inherits pseudo-variational upper bound character from its parent VCCD functional,

$$E_{\text{VCCD}} = \frac{\langle\Phi_0|e^{\hat{T}_2^\dagger}\hat{H}e^{\hat{T}_2}|\Phi_0\rangle}{\langle\Phi_0|e^{\hat{T}_2^\dagger}e^{\hat{T}_2}|\Phi_0\rangle} = \langle\Phi_0|e^{\hat{T}_2^\dagger}\hat{H}e^{\hat{T}_2}|\Phi_0\rangle_L, \tag{5}$$

which we have shown previously to be highly stabilizing, even upon the addition of perturbative corrections for the effects of higher excitations.[87,88] For the case of non-HF references, these perturbative corrections include the additional terms noted by Watts *et al.*,[93] making the method correct to fourth-order in perturbation theory.

The TCC methods, on the other hand, are defined through projection of the similarity-transformed Schrödinger equation onto the manifolds of singly, doubly and (if applicable) more highly excited determinants. For example, the equations for the CCSD method,

$$\langle\Phi_0|e^{-\hat{T}}\hat{H}e^{\hat{T}}|\Phi_0\rangle = E_{\text{CCSD}}, \tag{6}$$

$$\big\langle\Phi_i^a\big|e^{-\hat{T}}\hat{H}e^{\hat{T}}|\Phi_0\rangle = 0, \tag{7}$$

$$\big\langle\Phi_{ij}^{ab}\big|e^{-\hat{T}}\hat{H}e^{\hat{T}}|\Phi_0\rangle = 0, \tag{8}$$

and the closely related BCCD method,[92]

$$\langle\Phi_0|\hat{H}e^{\hat{T}_2}|\Phi_0\rangle = E_{\text{BCCD}}, \tag{9}$$

$$\big\langle\Phi_i^a\big|\hat{H}e^{\hat{T}_2}|\Phi_0\rangle = 0, \tag{10}$$

$$\big\langle\Phi_{ij}^{ab}\big|\hat{H}e^{\hat{T}_2}|\Phi_0\rangle = T_{ij}^{ab}E_{\text{BCCD}}, \tag{11}$$

are as above, with the following definition of the cluster operator:

$$\hat{T} = \hat{T}_1 + \hat{T}_2, \tag{12}$$

$$\hat{T}_1|\Phi_0\rangle = T_a^i\big|\Phi_i^a\big\rangle, \tag{13}$$

$$\hat{T}_2|\Phi_0\rangle = \tfrac{1}{4}T_{ab}^{ij}\big|\Phi_{ij}^{ab}\big\rangle. \tag{14}$$

Zero-frequency nonlinear optical properties may be calculated from any of these methods by finite-difference differentiation of the calculated energies with respect to the strength of a small applied field; if the molecular Hamiltonian is perturbed by the application of a weak electric field, $\mathcal{F}$, the total energy, E, of the molecule may be written as a Taylor series in orders of the field strength,[94]

$$E = \sum_{n=0}^{\infty}\frac{\mathcal{F}^n}{n!}\left.\frac{d^nE}{d\mathcal{F}^n}\right|_{\mathcal{F}=0}. \tag{15}$$

The dipole moment of the molecule in the direction of the applied field, a measure of the separation of charge in the molecule along that axis, is

$$\begin{aligned}\langle\mu\rangle &= -\frac{dE}{d\mathcal{F}}\\ &= -\sum_{n=1}^{\infty}\frac{\mathcal{F}^{n-1}}{(n-1)!}\left.\frac{d^nE}{d\mathcal{F}^n}\right|_{\mathcal{F}=0}.\end{aligned} \tag{16}$$

The first term in this series is the static (or permanent) dipole moment, and the other terms represent the contributions to the induced dipole moment. The coefficients of the second, third, and fourth terms, which measure the response of the molecule to an applied field, are the electric polarizability, α, the hyperpolarizability, β, and the second hyperpolarizability, γ:

$$\alpha = -\left.\frac{d^2E}{d\mathcal{F}^2}\right|_{\mathcal{F}=0}, \tag{17}$$

$$\beta = -\frac{1}{2!}\left.\frac{d^3E}{d\mathcal{F}^3}\right|_{\mathcal{F}=0}, \tag{18}$$

$$\gamma = -\frac{1}{3!}\left.\frac{d^4E}{d\mathcal{F}^4}\right|_{\mathcal{F}=0}. \tag{19}$$

III. METHODOLOGY

In this article, we benchmark the performance of QVCC against CCSD, CCSD(T), BCCD and BCCD(T) on several model hydrogen systems, using either full configuration interaction (FCI) or multireference averaged quadratic coupled cluster[69] (AQCC) as the standard for correct behaviour in each case. The sensitivity of the NLO properties, in particular, to the treatment of electron correlation in these systems make them perfect tests of any new quantum chemical method. In each case, a restricted Hartree-Fock (RHF) reference wavefunction is used. Although better results could possibly be achieved by the use of an unrestricted Hartree-Fock (UHF) reference wavefunction that correctly describes molecular dissociation, by instead using RHF in each case a fair comparison between each of the methods can be achieved. We compare and contrast the effectiveness of the RHF-based and UHF-based quantum chemical methods separately in Sec. IV G. Additionally, in order to further establish a fair benchmark of comparison between the methods, we substitute optimization of the orbitals in the QVCC calculations for the Brueckner condition, so that BQVCCD and BQVCCD(T) may be compared directly with BCCD and BCCD(T).

We assign each model system two degrees of freedom, and, in each case, we gain insight into how the properties of interest vary by examining 1D cuts of the potential energy surfaces or the surfaces of the polarizability or second hyperpolarizability. For several of the systems we also systematically gauge the accuracy of each of the single-reference electronic structure methods by obtaining a set of errors (computed by taking the value of the property of interest and subtracting from it the value obtained from a more accurate calculation, such as FCI, over a representative region of the corresponding potential energy surface. We also supply a supporting selection of FCI or MRAQCC energies, polarizabilities, and second hyperpolarizabilities for each of the models in order to allow the scale of the errors presented to be established. This is given in Table I.

TABLE I. Calculated energies, polarizabilities, and second hyperpolarizabilities for a selection of geometries of the various model hydrogen systems with the aug-cc-pVDZ basis. All quantities are in atomic units, and calculated with either the FCI (H_4) or MRAQCC (H_6) methods.

$D_{\infty h}$ H_4	R_1 (Å)	R_2 (Å)	E	α	γ
	1.00	1.00	−2.258545	$9.891 \times 10^{+0}$	$5.206 \times 10^{+1}$
	1.00	4.00	−2.283675	$1.158 \times 10^{+1}$	$5.107 \times 10^{+1}$
	2.00	1.75	−2.048722	$1.615 \times 10^{+1}$	$8.584 \times 10^{+1}$
	2.50	2.50	−2.008549	$1.673 \times 10^{+1}$	$1.072 \times 10^{+2}$
	3.00	4.00	−1.999858	$1.688 \times 10^{+1}$	$1.055 \times 10^{+2}$
C_{2v} H_4	R (Å)	θ (°)	E	α	γ
	2.25	0.0	−2.020093	$1.593 \times 10^{+1}$	$8.977 \times 10^{+1}$
	2.50	0.0	−2.009633	$1.626 \times 10^{+1}$	$1.016 \times 10^{+2}$
	2.75	0.0	−2.003707	$1.643 \times 10^{+1}$	$1.070 \times 10^{+2}$
	3.00	0.0	−2.000577	$1.653 \times 10^{+1}$	$1.075 \times 10^{+2}$
	3.25	0.0	−1.998985	$1.661 \times 10^{+1}$	$1.055 \times 10^{+2}$
D_{2h} H_4	R (Å)	θ (°)	E	α	γ
	1.75	80.0	−2.017706	$1.632 \times 10^{+1}$	$9.883 \times 10^{+1}$
	2.00	70.0	−2.016094	$1.668 \times 10^{+1}$	$1.050 \times 10^{+2}$
	2.00	80.0	−2.005927	$1.655 \times 10^{+1}$	$1.078 \times 10^{+2}$
	2.25	70.0	−2.005764	$1.675 \times 10^{+1}$	$1.084 \times 10^{+2}$
	2.25	80.0	−2.000833	$1.664 \times 10^{+1}$	$1.074 \times 10^{+2}$
C_{2h} H_4	R (Å)	θ (°)	E	α	γ
	1.0	45.0	−2.253203	$9.792 \times 10^{+0}$	$7.684 \times 10^{+1}$
	1.5	45.0	−2.130547	$1.441 \times 10^{+1}$	$6.347 \times 10^{+1}$
	2.0	45.0	−2.040944	$1.641 \times 10^{+1}$	$8.920 \times 10^{+1}$
	2.5	45.0	−2.008522	$1.671 \times 10^{+1}$	$1.068 \times 10^{+2}$
	3.0	45.0	−2.000026	$1.676 \times 10^{+1}$	$1.056 \times 10^{+2}$
$D_{\infty h}$ H_6	R_1 (Å)	R_2 (Å)	E	α	γ
	1.0	1.2	−3.400172	$1.471 \times 10^{+1}$	$6.743 \times 10^{+1}$
	1.2	1.8	−3.325041	$1.895 \times 10^{+1}$	$7.127 \times 10^{+1}$
	1.4	1.6	−3.234402	$2.065 \times 10^{+1}$	$7.499 \times 10^{+1}$
	1.6	1.6	−3.165001	$2.217 \times 10^{+1}$	$7.866 \times 10^{+1}$
	1.8	1.8	−3.105677	$2.370 \times 10^{+1}$	$8.935 \times 10^{+1}$

Although much of the interest in model hydrogen systems is in the NLO properties of linear chains parallel to the longitudinal axis, we relax this constraint and investigate several different model hydrogen systems. However, we first investigate only the perpendicular NLO properties of each of the model systems. We do this for several reasons. First, in each of the models that we test, there is a unique axis perpendicular to the plane of the system, whereas, for several of the models, no such unique axis exists in the plane. Thus, the perpendicular polarizabilities yield a single representative test for each system. Second, the perpendicular nonlinear optical properties are less sensitive to the applied field strength and are thus more amenable to calculation by finite-difference differentiation. Third, the polarizabilities perpendicular to a bond axis are interesting in their own right, since they give a measure of the shape of the electronic structure, and, in particular, the contraction of the electron distribution as atoms are brought together to form covalent bonds. Finally, it is our goal only to present further evidence that our new and robust electronic structure ansatz that performs pseudo-variationally for the calculation of potential energy curves allows the more accurate prediction of NLO properties when TCC fails to perform adequately, making it potentially valuable for future investigations, and perpendicular properties suffice for this.

Four of the model systems that we test are illustrated in Figure 1, which are, in clockwise order from the top-left, $D_{\infty h}$, C_{2v}, D_{2h}, and C_{2h} arrangements of four hydrogen atoms. We also investigate the 6-atom equivalent of the $D_{\infty h}$ model. We further establish that our findings extend to parallel polarizabilities and hyperpolarizabilities by investigating the

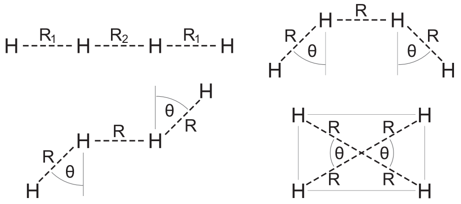

FIG. 1. Clockwise from top-left, the $D_{\infty h}$, C_{2v}, D_{2h}, and C_{2h} H_4 models.

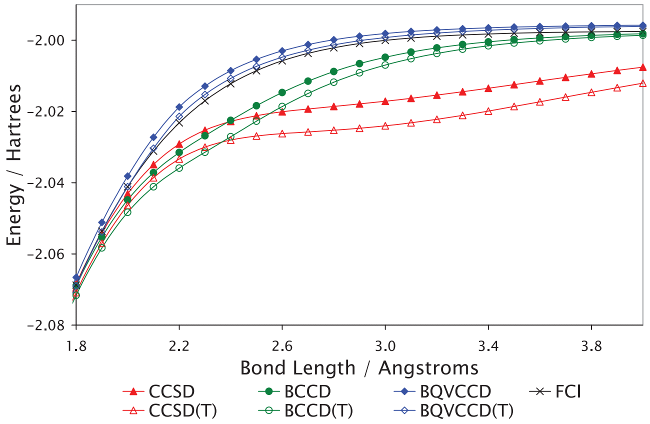

FIG. 2. Calculated energies of the $D_{\infty h}$ H_4 model with $R_1 = R_2$ and the aug-cc-pVDZ basis.

metal-insulator transition in $D_{\infty h}$ H_{10} as the nearest neighbour separation of the atoms is increased.

IV. RESULTS AND DISCUSSION

All calculations in this article were performed with the MOLPRO[95,96] quantum chemistry software package and most make use of the correlation-consistent basis sets of Dunning and co-workers[97] augmented with additional diffuse functions.[98]

A. The $D_{\infty h}$ H_4 model

The $D_{\infty h}$ H_4 model consists of four hydrogen atoms arranged linearly, with R_1 corresponding to the distance between the outer and inner atoms, and with R_2 corresponding to the distance between the two inner atoms, as is illustrated by the top-left diagram of Figure 1. For large R_2, the system corresponds to two isolated hydrogen molecules, each with bond length R_1, whereas for large R_1, the outer hydrogen atoms become isolated, leaving an inner hydrogen molecule with bond length R_2.

In Figure 2 we show how the energies vary for a uniform ($R_1 = R_2$) arrangement of the atoms as the common bond length is increased. In the case of the energy, BQVCCD clearly out-performs both CCSD and BCCD; the BQVCCD curve remains above FCI throughout, and the peak BQVCCD error, located around 2.2 Å, is significantly smaller in magnitude than the TCC peak errors. The BQVCCD curve also remains fairly parallel to the FCI curve, and the error therefore remains uniform throughout, whereas both CCSD and BCCD display large fluctuations in accuracy relative to FCI. Furthermore, it is apparent that the addition of the triples correction to BQVCCD improves the overall description of the potential energy curve, resulting in smaller errors throughout, whereas it has the opposite effect on the TCC methods, magnifying their errors.

An error analysis for the $D_{\infty h}$ H_4 model is given in Table II, and supports the observations already made. BQVCCD(T) possesses the smallest mean signed and mean absolute errors of the methods tested, and by roughly an order of magnitude in some cases. The standard deviation of the BQVCCD(T) energy errors is also the smallest of any of the methods, indicating that BQVCCD(T) maintains roughly the same level of accuracy over the potential energy surface, whereas the TCC methods are far less predictable or reliable.

The polarizability errors are similarly in favour of BQVCCD(T). The BQVCCD(T) mean signed error is, at 50 μa.u., at least two orders of magnitude smaller than any of the TCC values, and the mean absolute errors are between 3 and 4 times smaller than the values predicted by BCCD, the best of the TCC methods in this case. Of all the methods tested, BQVCCD(T) predicts the second hyperpolarizabilities closest in value to FCI, with a mean absolute error at least 3 times smaller than both CCSD and BCCD.

TABLE II. Errors relative to FCI for calculated energies of, and polarizabilities perpendicular to the $D_{\infty h}$ H_4 model with the aug-cc-pVDZ basis. Results were obtained from the set of points $\{(R_1, R_2)\}$, where $R_1 \in \{1.0, 1.5, 2.0, 2.5, 3.0\}$Å and $R_2 \in \{1.0, 1.75, 2.5, 3.25, 4.0\}$Å.[a]

		CCSD	CCSD(T)	BCCD	BCCD(T)	BQVCCD	BQVCCD(T)
E	$\bar{\epsilon}$	-3.42×10^{-3}	-6.61×10^{-3}	-1.20×10^{-3}	-2.96×10^{-3}	1.87×10^{-3}	5.24×10^{-4}
	$\lvert\bar{\epsilon}\rvert$	4.49×10^{-3}	6.65×10^{-3}	2.33×10^{-3}	3.01×10^{-3}	1.87×10^{-3}	7.07×10^{-4}
	σ	9.56×10^{-3}	1.34×10^{-2}	5.45×10^{-3}	7.44×10^{-3}	2.31×10^{-3}	1.11×10^{-3}
α	$\bar{\epsilon}$	-1.80×10^{-1}	-2.36×10^{-1}	1.43×10^{-2}	3.25×10^{-2}	-3.04×10^{-3}	-5.76×10^{-5}
	$\lvert\bar{\epsilon}\rvert$	1.82×10^{-1}	2.49×10^{-1}	1.02×10^{-1}	1.24×10^{-1}	4.17×10^{-2}	3.06×10^{-2}
	σ	3.97×10^{-1}	5.51×10^{-1}	3.00×10^{-1}	3.81×10^{-1}	8.89×10^{-2}	7.12×10^{-2}
γ	$\bar{\epsilon}$	6.56×10^{-1}	-7.40×10^{-1}	$2.06 \times 10^{+0}$	$1.25 \times 10^{+0}$	7.43×10^{-1}	4.53×10^{-1}
	$\lvert\bar{\epsilon}\rvert$	$4.43 \times 10^{+0}$	$5.24 \times 10^{+0}$	$3.74 \times 10^{+0}$	$3.67 \times 10^{+0}$	$1.12 \times 10^{+0}$	$1.11 \times 10^{+0}$
	σ	$9.82 \times 10^{+0}$	$1.11 \times 10^{+1}$	$1.02 \times 10^{+1}$	$1.02 \times 10^{+1}$	$1.48 \times 10^{+0}$	$1.74 \times 10^{+0}$

[a] Quoted values are the mean signed error, $\bar{\epsilon}$, the mean absolute error, $\lvert\bar{\epsilon}\rvert$, and the standard deviation of the signed errors, σ.

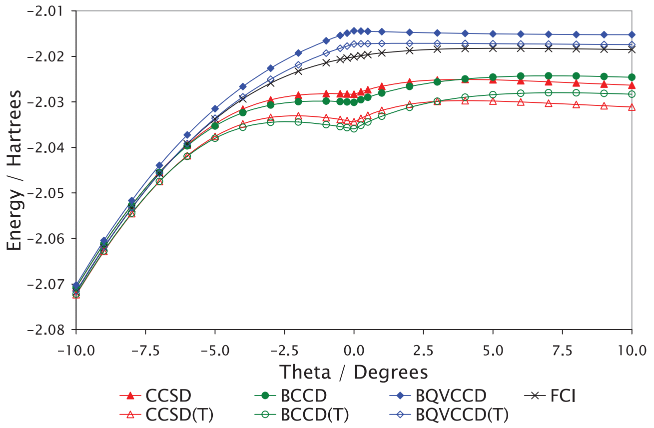

FIG. 3. Calculated potential energy curves for the C_{2v} H_4 model with $R = 2.25$ Å, and with the aug-cc-pVDZ basis.

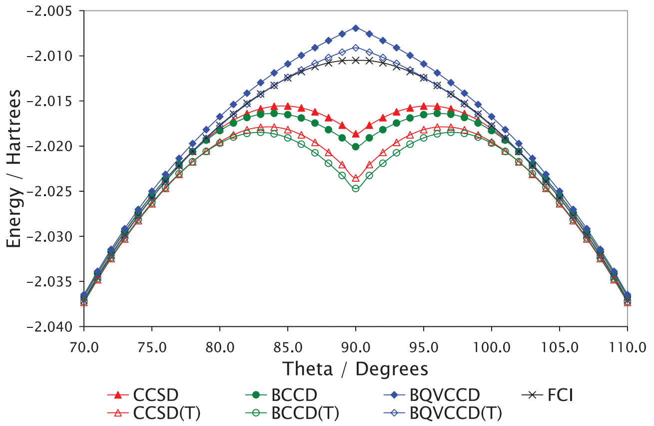

FIG. 4. Calculated potential energy curves for the D_{2h} H_4 model with $R = 1.75$ Å, and with the aug-cc-pVDZ basis.

B. The C_{2v} H_4 model

The C_{2v} model, illustrated by the diagram in the top-right of Figure 1, corresponds to a *cis* arrangement of the four hydrogen atoms, with the degrees of freedom chosen to be the distance between nearest neighbours and the angle subtended by lines from an outer atom to an inner atom and along the perpendicular to the line joining the two inner atoms.

The most interesting degree of freedom to vary in this system is the angle θ; the outer hydrogen atoms are nearby for $\theta < 0°$, but as the system is distorted through $\theta = 0°$, corresponding to the square geometry, the outer atoms swing apart and the optimum Hartree-Fock reference wavefunction changes. This results in cusps in the potential energy curves predicted by the single-reference methods at $\theta = 0°$, as can be seen in Figure 3. The CCSD and BCCD methods level off too quickly, forming concave cusps, whereas the BQVCCD cusp is convex and the curve mimics the FCI shape more correctly overall. It is again true that the (T) correction to the BQVCCD method results in an improved curve, even flattening the cusp, whereas the (T) correction to the TCC methods push the curves further from FCI quality and sharpen the cusps.

The error analysis for C_{2v} H_4 is given in Table III. As can be expected from the plot, the BQVCCD(T) method possesses the smallest errors in the calculated energies across all the categories. It is particularly striking that the BQVCCD(T) mean absolute error, at 0.4 millihartrees, is 25 times smaller than the CCSD(T) error, at 11 millihartrees, and 15 times smaller than the BCCD(T) value, at 7 millihartrees.

The polarizability errors are also quite impressive; the BQVCCD(T) mean absolute error for the perpendicular polarizability is 0.025 a.u., whereas the CCSD(T) and BCCD(T) errors are larger by factors of approximately 13 and 5, respectively. The standard deviations of the polarizability errors are also roughly an order of magnitude smaller for BQVCCD and BQVCCD(T) than for the TCC methods. The BCCD method predicts just slightly better second hyperpolarizability values than BQVCCD for this system, as measured by mean absolute errors. However, the standard deviation of the errors indicates that the BQVCCD method still has the smallest spread of errors, so that it remains the most reliable method for calculating second hyperpolarizabilities, despite its slightly poorer mean accuracy here.

C. The D_{2h} H_4 model

Next, we examine the D_{2h} H_4 model,[79] shown in the bottom-right of Figure 1, in which four hydrogen atoms are arranged in a rectangle that can be defined by the parameters R, which controls the distance of each H atom from the centre of mass, and θ, the angle subtended at the centre of mass by radii to two neighbouring vertices of the rectangle.

TABLE III. Errors relative to FCI for calculated energies, and polarizabilities perpendicular to the plane, in the C_{2v} H_4 model with the aug-cc-pVDZ basis. Results were obtained from the set of points $\{(R, \theta)\}$, where $R \in \{2.25, 2.5, 2.75, 3.0, 3.25\}$Å and $\theta \in \{0, \pm 2, \pm 4, \pm 6, \pm 8\}°$.

		CCSD	CCSD(T)	BCCD	BCCD(T)	BQVCCD	BQVCCD(T)
E	$\bar{\epsilon}$	-7.14×10^{-3}	-1.12×10^{-2}	-4.28×10^{-3}	-6.81×10^{-3}	1.65×10^{-3}	1.68×10^{-4}
	$\lvert\bar{\epsilon}\rvert$	7.17×10^{-3}	1.12×10^{-2}	4.32×10^{-3}	6.81×10^{-3}	1.65×10^{-3}	4.35×10^{-4}
	σ	6.10×10^{-3}	8.18×10^{-3}	2.68×10^{-3}	3.70×10^{-3}	1.12×10^{-3}	6.62×10^{-4}
α	$\bar{\epsilon}$	-1.45×10^{-1}	-2.48×10^{-1}	1.87×10^{-2}	4.33×10^{-2}	-3.25×10^{-2}	-1.89×10^{-2}
	$\lvert\bar{\epsilon}\rvert$	2.32×10^{-1}	3.29×10^{-1}	9.78×10^{-2}	1.18×10^{-1}	3.26×10^{-2}	2.48×10^{-2}
	σ	2.77×10^{-1}	3.88×10^{-1}	1.16×10^{-1}	1.35×10^{-1}	2.91×10^{-2}	3.00×10^{-2}
γ	$\bar{\epsilon}$	$3.32 \times 10^{+0}$	$5.11 \times 10^{+0}$	$-1.05 \times 10^{+0}$	$-2.28 \times 10^{+0}$	$1.75 \times 10^{+0}$	$1.72 \times 10^{+0}$
	$\lvert\bar{\epsilon}\rvert$	$5.23 \times 10^{+0}$	$6.84 \times 10^{+0}$	$1.57 \times 10^{+0}$	$2.60 \times 10^{+0}$	$1.77 \times 10^{+0}$	$1.79 \times 10^{+0}$
	σ	$6.36 \times 10^{+0}$	$8.47 \times 10^{+0}$	$1.81 \times 10^{+0}$	$2.58 \times 10^{+0}$	$1.37 \times 10^{+0}$	$2.04 \times 10^{+0}$

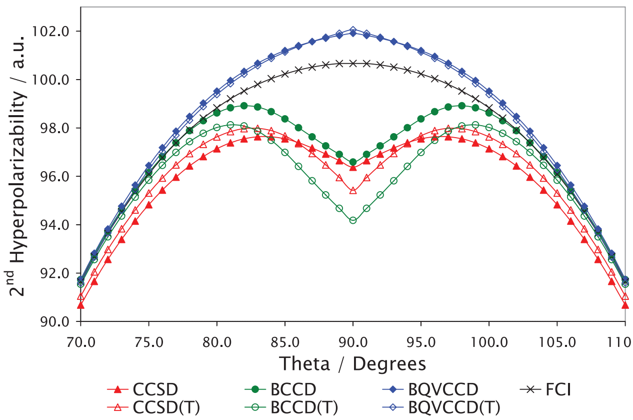

FIG. 5. Calculated second hyperpolarizabilities perpendicular to the plane of the D_{2h} H_4 model with $R = 1.75$ Å, and with the aug-cc-pVDZ basis

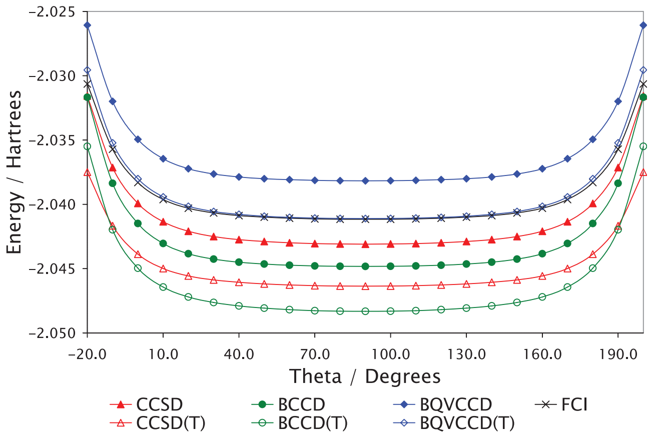

FIG. 6. Calculated potential energy curves for the C_{2h} H_4 model with $R = 2.0$ Å, and with the aug-cc-pVDZ basis.

The system is symmetric about $\theta = 90^\circ$, and the optimum Hartree-Fock reference wavefunction differs on either side of this line. Thus, the Hartree-Fock approximation breaks down around $\theta = 90^\circ$ as two determinants become equally important to the description of the ground-state electronic structure, and this makes the system an excellent test of single-reference post-Hartree-Fock electron correlation methods.

We have previously shown that the QVCCD method mimics the behaviour of VCCD (and thus FCI) well in this system,[71] and the improved shape of the potential energy curve relative to the TCC methods around the square geometry can be seen in Figure 4. However, the BQVCCD method additionally models the nonlinear optical properties of this system extremely well, achieving the correct shape for the second hyperpolarizability around $\theta = 90^\circ$ despite a displacement in the curve position, as can be seen in Figure 5. The cusp present in the BQVCCD and BQVCCD(T) potential energy curves has also almost vanished in the second hyperpolarizability curves. In contrast, the poor quality of the CCSD and BCCD methods in the interval [80°, 100°] that is apparent in the calculated energies deteriorates even further for this more challenging property, with CCSD, CCSD(T), BCCD, and BCCD(T) all predicting curves with incorrect slope relative to FCI, and possessing even sharper cusps.

As measured by the mean absolute error data presented in Table IV, it is clear that BQVCCD(T) predicts the potential energy curves and second hyperpolarizabilities that best approximate the FCI values overall, and that BQVCCD predicts the best polarizabilities. Similarly, the BQVCCD and BQVCCD(T) standard deviations are smaller than the equivalent TCC values, from which we infer that not only are the accuracies of BQVCCD-calculated energies, polarizabilities and second hyperpolarizabilities greatly improved, but that the calculations are also stabilized, resulting in more systematically predictable, consistent errors.

D. The C_{2h} H_4 model

The C_{2h} model is a simple modification of the C_{2v} model such that one of the outer hydrogens is on the opposite side, forming a trans structure. The diagram is given in the bottom-left of Figure 1. Increasing the angle θ causes the outer hydrogen atoms to swap to opposite sides, with $\theta = 90^\circ$ corresponding to linear geometry.

A plot of the potential energy curves obtained by varying the angle θ is shown in Figure 6. Both the CCSD and BCCD curves lie below FCI throughout, and the effect of the (T) correction is to push the curves lower still, further from FCI. However, the BQVCCD curve lies significantly above the FCI curve throughout, and the effect of the correction remains to push the energy down, resulting in the BQVCCD(T) curve being almost coincident with FCI. The calculated

TABLE IV. Errors relative to FCI for calculated energies of, and polarizabilities perpendicular to the D_{2h} H_4 model with the aug-cc-pVDZ basis. Results were obtained from the set of points $\{(R, \theta)\}$, where $R \in \{1.0, 1.75, 2.0, 2.25\}$Å and $\theta \in \{70, 72, 74, 76, 78, 80, 82, 84, 86, 87, 88, 89\}^\circ$.

		CCSD	CCSD(T)	BCCD	BCCD(T)	BQVCCD	BQVCCD(T)
E	$\bar{\epsilon}$	-7.69×10^{-4}	-2.59×10^{-3}	-1.09×10^{-3}	-2.83×10^{-3}	1.36×10^{-3}	2.89×10^{-5}
	$\bar{\lvert\epsilon\rvert}$	1.85×10^{-3}	2.63×10^{-3}	2.16×10^{-3}	2.89×10^{-3}	1.36×10^{-3}	3.01×10^{-4}
	σ	2.51×10^{-3}	3.03×10^{-3}	2.87×10^{-3}	3.39×10^{-3}	1.18×10^{-3}	3.99×10^{-4}
α	$\bar{\epsilon}$	4.36×10^{-2}	2.92×10^{-2}	8.18×10^{-3}	1.79×10^{-2}	-1.53×10^{-2}	-1.37×10^{-2}
	$\bar{\lvert\epsilon\rvert}$	6.33×10^{-2}	5.74×10^{-2}	4.71×10^{-2}	5.68×10^{-2}	2.35×10^{-2}	2.46×10^{-2}
	σ	7.85×10^{-2}	8.55×10^{-2}	6.88×10^{-2}	8.58×10^{-2}	3.09×10^{-2}	3.51×10^{-2}
γ	$\bar{\epsilon}$	$-1.07 \times 10^{+0}$	-6.49×10^{-1}	-2.04×10^{-1}	-7.80×10^{-1}	9.81×10^{-1}	7.74×10^{-1}
	$\bar{\lvert\epsilon\rvert}$	$1.59 \times 10^{+0}$	$1.09 \times 10^{+0}$	9.08×10^{-1}	$1.27 \times 10^{+0}$	9.88×10^{-1}	8.18×10^{-1}
	σ	$1.61 \times 10^{+0}$	$1.49 \times 10^{+0}$	$1.41 \times 10^{+0}$	$1.79 \times 10^{+0}$	7.92×10^{-1}	7.42×10^{-1}

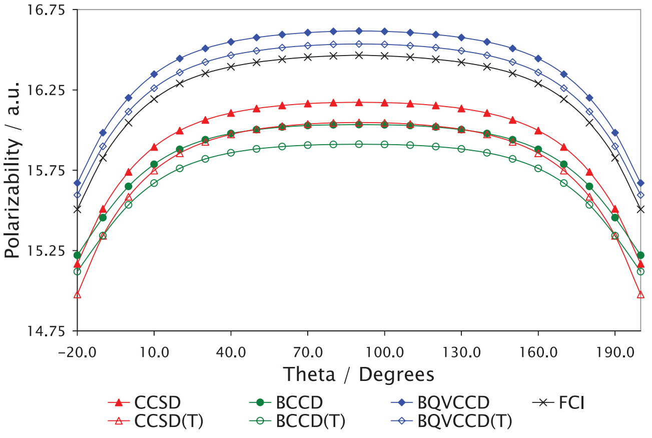

FIG. 7. Calculated polarizabilities perpendicular to the plane of the C_{2h} H_4 model with $R = 2.0$ Å, and with the aug-cc-pVDZ basis.

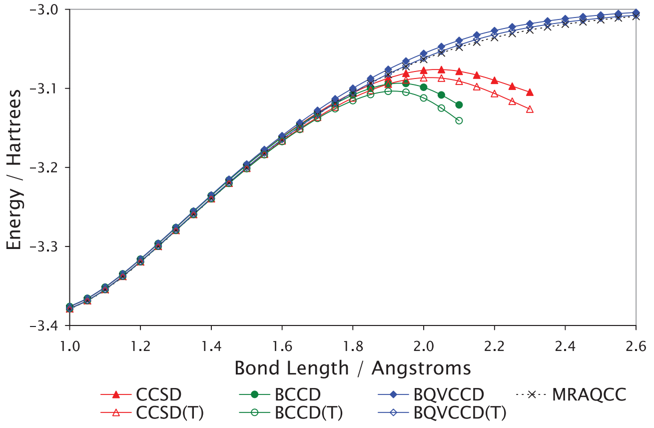

FIG. 8. Calculated potential energy curves for the $D_{\infty h}$ H_6 model with $R_1 = R_2$ and with the aug-cc-pVDZ basis.

polarizabilities are also shown in Figure 7, and although each of the methods deteriorates in quality for the calculation of this more difficult property, BQVCCD(T) remains in extremely good agreement with FCI throughout.

These graphs add credence to the error analysis presented in Table V, which indicates that BQVCCD(T) performs best for each of the properties and by almost all error measures. For example, the BQVCCD(T) mean absolute energy error is 16 and 9 times smaller than the CCSD(T) and BCCD(T) errors, respectively. The polarizabilities and second hyperpolarizabilities are similarly impressive, with errors 13 and 7 times smaller for the polarizabilities and by 5 and 4 times for the second hyperpolarizabilities, respectively.

E. The $D_{\infty h}$ H_6 model

Analogous to the $D_{\infty h}$ H_4 model, we have also studied the more severe test case of the $D_{\infty h}$ H_6 model in which six hydrogen atoms are arranged linearly, with bond lengths alternating as R_1, R_2, R_1, R_2, R_1.

First, we investigated the line along the potential energy surface defined by $R_1 = R_2$, for which the potential energy curves are given in Figure 8. All methods perform similarly well until approximately 1.6 Å. At this bond length, the TCC methods begin to degrade significantly in quality, dropping below the MRAQCC energy in a non-variational fashion. However, the BQVCCD and BQVCCD(T) energies, supported by the approximately fulfilled upper bound property, remain in excellent agreement with MRAQCC throughout and do not appear to degrade at all.

These findings extend also to the perpendicular polarizabilities, given in Figure 9, and second hyperpolarizabilities, given in Figure 10. The TCC methods predict a decreasing polarizability from approximately 1.8 Å, which is clearly at odds with the smooth and monotonically increasing MRAQCC polarizability. The BQVCCD predicted polarizabilities, on the other hand, are far superior, and although the polarizability decreases around 2.2 Å, this is quickly corrected such that the BQVCCD curve remains near the MRAQCC curve throughout. The second hyperpolarizabilities are even more striking, with the TCC methods predicting values several times too large for 1.8–2.2 Å. The BQVCCD curves again experience crossings with the MRAQCC curve, but the predicted values remain quantitatively accurate at all points.

The error analysis for this system is given in Table VI. An examination of the mean absolute errors for each of the three properties confirms that BQVCCD(T) is the most accurate of the single-reference methods, and by an order of magnitude in each case. The standard deviations also attest the reliability of the BQVCCD(T) method, with CCSD values factors of 5, 8, and 8 worse for the energy, polarizability, and second hyperpolarizability, respectively. Finally, we note once again,

TABLE V. Errors relative to FCI for calculated energies of, and polarizabilities perpendicular to the C_{2h} H_4 model with the aug-cc-pVDZ basis. Results were obtained from the set of points $\{(R, \theta)\}$, where $R \in \{1.0, 1.5, 2.0, 2.5, 3.0\}$Å and $\theta \in \{-15, 0, 15, 30, 45, 60, 75, 90\}°$.

		CCSD	CCSD(T)	BCCD	BCCD(T)	BQVCCD	BQVCCD(T)
E	$\bar{\epsilon}$	-6.31×10^{-3}	-1.04×10^{-2}	-2.97×10^{-3}	-5.53×10^{-3}	2.45×10^{-3}	6.55×10^{-4}
	$\lvert\bar{\epsilon}\rvert$	7.54×10^{-3}	1.05×10^{-2}	4.13×10^{-3}	5.64×10^{-3}	2.45×10^{-3}	6.55×10^{-4}
	σ	8.70×10^{-3}	1.13×10^{-2}	4.25×10^{-3}	5.30×10^{-3}	8.43×10^{-4}	5.57×10^{-4}
α	$\bar{\epsilon}$	-2.57×10^{-1}	-3.78×10^{-1}	-4.57×10^{-2}	-5.20×10^{-2}	1.31×10^{-2}	1.33×10^{-3}
	$\lvert\bar{\epsilon}\rvert$	2.58×10^{-1}	3.78×10^{-1}	1.33×10^{-1}	1.79×10^{-1}	5.23×10^{-2}	2.74×10^{-2}
	σ	2.66×10^{-1}	3.68×10^{-1}	2.02×10^{-1}	2.68×10^{-1}	7.46×10^{-2}	3.80×10^{-2}
γ	$\bar{\epsilon}$	4.67×10^{-1}	-3.17×10^{-1}	7.54×10^{-1}	-2.97×10^{-1}	-2.03×10^{-1}	-2.84×10^{-1}
	$\lvert\bar{\epsilon}\rvert$	$6.87 \times 10^{+0}$	$9.08 \times 10^{+0}$	$6.14 \times 10^{+0}$	$7.63 \times 10^{+0}$	$2.14 \times 10^{+0}$	$1.95 \times 10^{+0}$
	σ	$1.00 \times 10^{+1}$	$1.36 \times 10^{+1}$	$8.77 \times 10^{+0}$	$1.13 \times 10^{+1}$	$2.91 \times 10^{+0}$	$2.78 \times 10^{+0}$

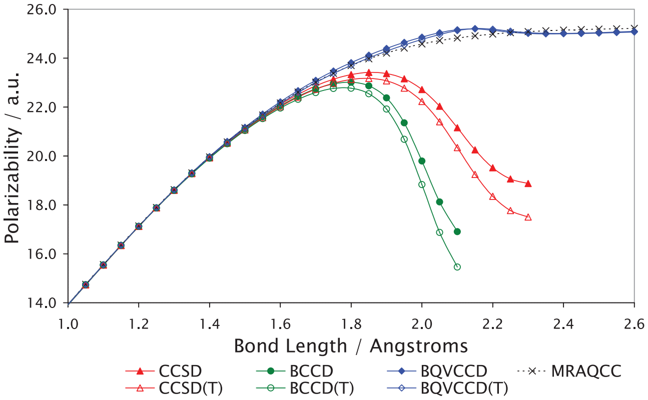

FIG. 9. Calculated polarizabilities for the $D_{\infty h}$ H_6 model with $R_1 = R_2$ and with the aug-cc-pVDZ basis.

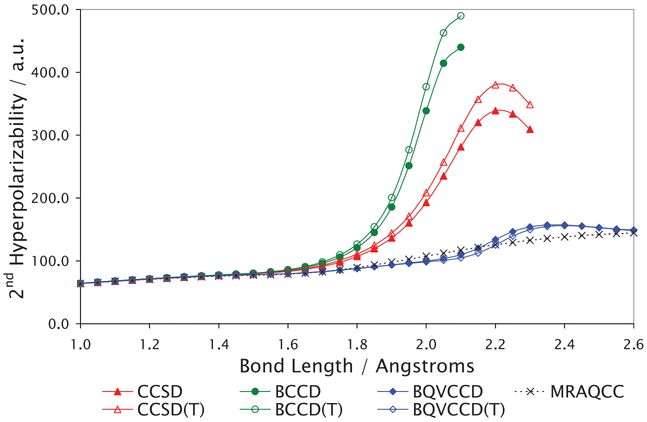

FIG. 10. Calculated second hyperpolarizabilities for the $D_{\infty h}$ H_6 model with $R_1 = R_2$ and with the aug-cc-pVDZ basis.

that, for this set of data, the addition of the (T) correction to the BQVCCD method yields smaller errors overall, whereas its addition to the TCC methods tends to have the opposite effect.

F. Towards the metal-insulator transition: H_{10}

As a last example, we examine the NLO properties *parallel* to the $D_{\infty h}$ H_{10} model system as a function of the separation between sites. Thus, this example is used to investigate whether our extremely positive findings for the calculation of perpendicular polarizabilities using the BQVCCD and BQVCCD(T) methods are reflected in parallel polarizabilities also. The H_{10} system, along with other hydrogen chains of similar length, have been investigated previously in the context of metal-insulator transitions, for example in Ref. 99. In order to closely reproduce the results of this article, and in order to make the FCI calculations practical, we have made use of the minimal STO-3G basis set, rendering the calculated polarizabilities of qualitative validity only.

The calculated energies for this system are given in Figure 11, and polarizabilities in Figure 12, in which it is clear that each of the methods is capable of describing the short bond length region (the region of increasing slope), where the system is thought to be metallic, but the methods based on TCC struggle in the region of decreasing slope of the polarizability, becoming catastrophically incorrect around a bond length of 1.5 Å. The BQVCCD and BQVCCD(T) methods, however, are in good agreement with FCI throughout, despite underestimating the value of the polarizability itself. Thus, not only is the BQVCCD ansatz similarly impressive for the evaluation of parallel polarizabilities, but this example illustrates an application of the method to a metal-insulator transition; a problem of widespread interest. For completeness, we have also included a plot of the second hyperpolarizability parallel to the longitudinal axis of the molecule in Figure 13, with shows similar accuracy.

G. Comparison with UHF-CCSD

Finally, as we have already noted, all calculations presented so far have used RHF reference wavefunctions. However, very good results for these model systems can be obtained at extended interatomic distances by the use of a UHF reference wavefunction, which, unlike the RHF wavefunction, is qualitatively correct at dissociation; in RHF theory, the α and β electrons are constrained to occupy the same spatial orbitals. If a molecule dissociates into open-shell fragments, which should be uncharged on physical grounds, this restriction necessarily leads to ionic contamination of the wavefunction as the molecule dissociates.[100] In UHF theory, this constraint is relaxed.

TABLE VI. Errors relative to MRAQCC for calculated energies of, and polarizabilities perpendicular to the $D_{\infty h}$ H_6 model with the aug-cc-pVDZ basis. Results were obtained from the set of points $\{(R_1, R_2)\}$, where $R_1, R_2 \in \{1.0, 1.2, 1.4, 1.6, 1.8\}$Å.

		CCSD	CCSD(T)	BCCD	BCCD(T)	BQVCCD	BQVCCD(T)
E	$\bar{\epsilon}$	3.03×10^{-3}	-4.09×10^{-3}	2.54×10^{-3}	-3.29×10^{-3}	5.42×10^{-3}	1.12×10^{-4}
	$\lvert\bar{\epsilon}\rvert$	3.52×10^{-3}	4.33×10^{-3}	3.74×10^{-3}	3.53×10^{-3}	5.42×10^{-3}	5.57×10^{-4}
	σ	3.03×10^{-3}	6.65×10^{-3}	3.97×10^{-3}	6.24×10^{-3}	3.77×10^{-3}	6.29×10^{-4}
α	$\bar{\epsilon}$	-1.35×10^{-1}	-2.35×10^{-1}	-1.61×10^{-1}	-2.16×10^{-1}	9.16×10^{-3}	-2.40×10^{-2}
	$\lvert\bar{\epsilon}\rvert$	1.36×10^{-1}	2.35×10^{-1}	1.61×10^{-1}	2.18×10^{-1}	4.20×10^{-2}	2.50×10^{-2}
	σ	2.36×10^{-1}	3.79×10^{-1}	3.32×10^{-1}	4.56×10^{-1}	6.07×10^{-2}	3.13×10^{-2}
γ	$\bar{\epsilon}$	$5.74 \times 10^{+0}$	$5.82 \times 10^{+0}$	$6.23 \times 10^{+0}$	$5.90 \times 10^{+0}$	9.74×10^{-1}	1.09×10^{-1}
	$\lvert\bar{\epsilon}\rvert$	$5.74 \times 10^{+0}$	$6.43 \times 10^{+0}$	$6.24 \times 10^{+0}$	$6.62 \times 10^{+0}$	$1.13 \times 10^{+0}$	7.70×10^{-1}
	σ	$9.79 \times 10^{+0}$	$1.21 \times 10^{+1}$	$1.35 \times 10^{+1}$	$1.61 \times 10^{+1}$	$1.19 \times 10^{+0}$	$1.20 \times 10^{+0}$

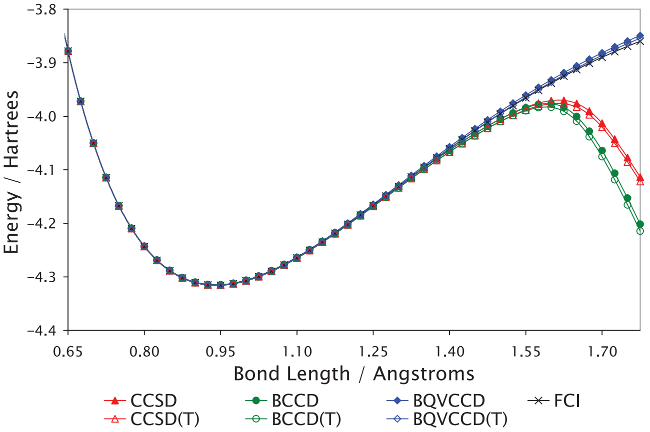

FIG. 11. Calculated energies of the $D_{\infty h}$ H_{10} model with $R_1 = R_2$ and the STO-3G basis.

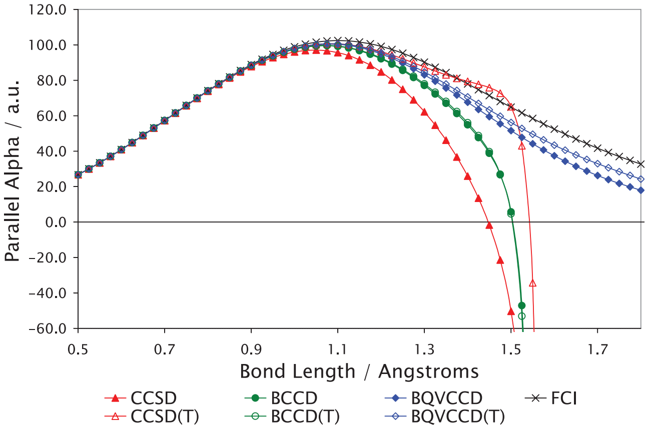

FIG. 12. Calculated longitudinal polarizabilities of the $D_{\infty h}$ H_{10} model with $R_1 = R_2$ and the STO-3G basis.

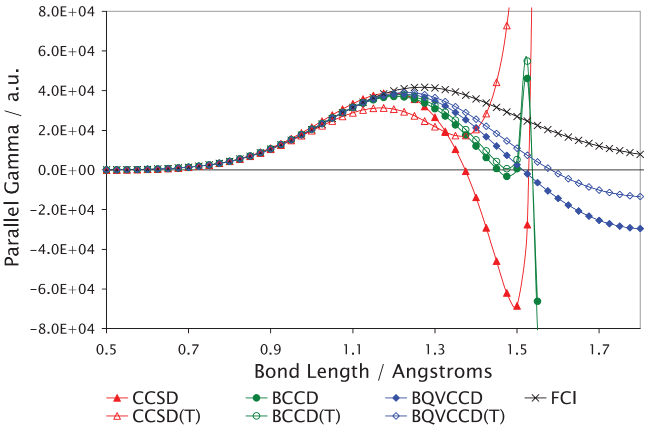

FIG. 13. Calculated longitudinal second hyperpolarizabilities of the $D_{\infty h}$ H_{10} model with $R_1 = R_2$ and the STO-3G basis.

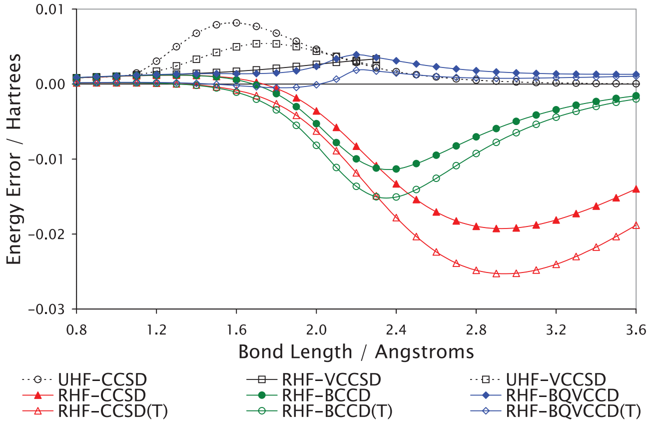

FIG. 14. Errors relative to FCI for calculated energies of the $D_{\infty h}$ H_4 model with $R_1 = R_2$ and the cc-pVDZ basis.

Thus, it is of interest to explore whether our pseudo-variational method that appears to predict quantitatively accurate potential energy curves for these models produces results comparable to a UHF-based post-Hartree-Fock method. In order to assess this, we performed additional UHF-CCSD calculations on the $D_{\infty h}$ H_4 model. Our results, illustrated in Figure 14, are quite surprising; as is to be expected, the UHF-CCSD results are in agreement with the RHF-CCSD results at short bond lengths and approach FCI quality at dissociation, but there are large errors in the interval 1.2–2.4 Å. This can be ascribed to spin contamination effects.[101,102] In contrast, an RHF wavefunction is always an eigenfunction of $\hat{S}^2$, so that the RHF-CCSD and RHF-BQVCCD methods yield exact spin eigenstates, and therefore have the advantage over UHF-CCSD that they do not suffer from spin contamination. However, while RHF-CCSD diverges at sufficiently long bond lengths, RHF-BQVCCD displays an accuracy rivalling UHF-CCSD and even exceeding it over regions of the potential energy curve, despite the fact that the reference wavefunction becomes qualitatively wrong. This suggests the closed-shell-reference QVCC approach to be generally useful and applicable to problems in which a correct treatment of dissociation is required and a wavefunction that is a spin eigenfunction would also be desirable. In addition, it is clear that UHF-VCC mitigates the effects of spin contamination in comparison to UHF-TCC, and this has been noted previously.[80] This gives impetus to the further development of a UHF-QVCC theory.

V. CONCLUDING REMARKS

We have provided the results of benchmark calculations on several prototypical multiradical model hydrogen systems. As we and others have demonstrated previously, when the single-determinantal Hartree-Fock approximation is a poor description of the exact electronic structure, as occurs in these examples, the traditional coupled cluster method can perform badly, predicting unstable potential energy curves that may even collapse non-variationally to energies significantly below FCI. However, the quasi-variational coupled cluster method, in which an upper bound on the exact ground-state Schrödinger energy eigenvalue is approximately preserved at the cost of no other methodological property, demonstrates remarkable stability in situations where TCC predicts unphysical results. Our previous studies have demonstrated this to be particularly relevant for the single-reference description of problems involving the breaking of multiple bonds, and the present study additionally indicates that our method may be useful in the investigation of singlet multiradical systems.

Furthermore, our results demonstrate that the property of an approximate variational upper bound on the energy does not simply improve the calculated energies themselves, but in fact yields a more robust description of the overall electronic structure when static correlation is problematic, leading to enhanced stability for the calculation of electrical response properties as well. This may be compared and likened with our previous observation that by successfully capturing the non-dynamic correlation, indirect improvements in the stability of approximate corrections for triple excitations based upon perturbation theory also emerge.[87,88] Thus, it is unfortunate that the current generation of single-reference *ab initio* electronic structure methods has largely abandoned the property of a variational upper bound in order to achieve rigorous extensivity and an exact treatment of limiting systems because our work demonstrates that this extremely powerful property should not, and indeed need not, be entirely sacrificed.

[1] H. Nalwa and S. Miyata, *Nonlinear Optics of Organic Molecules and Polymers*, 1st ed. (CRC, 1997).

[2] B. H. Cumpston, S. P. Ananthavel, S. Barlow, D. L. Dyer, J. E. Ehrlich, L. L. Erskine, A. A. Heikal, S. M. Kuebler, I.-Y. S. Lee, D. McCord-Maughon, J. Qin, H. Rl, M. Rumi, X.-L. Wu, S. R. Marder, and J. W. Perry, Nature (London) **398**, 51 (1999).

[3] S. Kawata, H.-B. Sun, T. Tanaka, and K. Takada, Nature (London) **412**, 697 (2001).

[4] M. Albota, D. Beljonne, J.-L. Brédas, J. E. Ehrlich, J.-Y. Fu, A. A. Heikal, S. E. Hess, T. Kogej, M. D. Levin, S. R. Marder, D. McCord-Maughon, J. W. Perry, H. Rckel, M. Rumi, G. Subramaniam, W. W. Webb, X.-L. Wu, and C. Xu, Science **281**, 1653 (1998).

[5] W. Zhou, S. M. Kuebler, K. L. Braun, T. Yu, J. K. Cammack, C. K. Ober, J. W. Perry, and S. R. Marder, Science **296**, 1106 (2002).

[6] W. R. Dichtel, J. M. Serin, C. Edder, J. M. J. Frchet, M. Matuszewski, L.-S. Tan, T. Y. Ohulchanskyy, and P. N. Prasad, J. Am. Chem. Soc. **126**, 5380 (2004).

[7] F. Terenziani, C. Katan, E. Badaeva, S. Tretiak, and M. Blanchard-Desce, Adv. Mater. **20**, 4641 (2008).

[8] Z. Li, S. Xu, L. Huang, X. Huang, L. Niu, Z. Chen, Z. Zhang, F. Zhang, and K. Kasatani, Chem. Phys. Lett. **441**, 123 (2007).

[9] W. Zhao, J. Phys. Chem. Lett. **2**, 482 (2011).

[10] M. Samoc, G. T. Dalton, J. A. Gladysz, Q. Zheng, Y. Velkov, H. Agren, P. Norman, and M. G. Humphrey, Inorg. Chem. **47**, 9946 (2008).

[11] R. Zalesny, O. Loboda, K. Iliopoulos, G. Chatzikyriakos, S. Couris, G. Rotas, N. Tagmatarchis, A. Avramopoulos, and M. G. Papadopoulos, Phys. Chem. Chem. Phys. **12**, 373 (2010).

[12] S. Ohira, J. M. Hales, K. J. Thorley, H. L. Anderson, J. W. Perry, and J.-L. Brédas, J. Am. Chem. Soc. **131**, 6099 (2009).

[13] H. Reis, O. Loboda, A. Avramopoulos, M. G. Papadopoulos, B. Kirtman, J. M. Luis, and R. Zalesny, J. Comput. Chem. **32**, 908 (2011).

[14] R. Orlando, R. Bast, K. Ruud, U. Ekstrm, M. Ferrabone, B. Kirtman, and R. Dovesi, J. Phys. Chem. A **115**, 12631 (2011).

[15] S. R. Marder, C. B. Gorman, B. G. Tiemann, J. W. Perry, G. Bourhill, and K. Mansour, Science **261**, 186 (1993).

[16] F. Meyers, S. R. Marder, B. M. Pierce, and J. L. Bredas, J. Am. Chem. Soc. **116**, 10703 (1994).

[17] J. L. Bredas, C. Adant, P. Tackx, A. Persoons, and B. M. Pierce, Chem. Rev. **94**, 243 (1994).

[18] R. R. Tykwinski, U. Gubler, R. E. Martin, F. Diederich, C. Bosshard, and G. Peter, J. Phys. Chem. B **102**, 4451 (1998).

[19] B. Champagne and E. A. Perpete, Int. J. Quantum Chem. **75**, 441 (1999).

[20] B. Champagne, E. A. Perpete, D. Jacquemin, S. J. A. van Gisbergen, E.-J. Baerends, C. Soubra-Ghaoui, K. A. Robins, and B. Kirtman, J. Phys. Chem. A **104**, 4755 (2000).

[21] S. Borini, P. A. Limacher, and H. P. Luthi, J. Chem. Phys. **131**, 124105 (2009).

[22] M. de Wergifosse and B. Champagne, J. Chem. Phys. **134**, 074113 (2011).

[23] M. Nakano, T. Minami, R. Kishi, Y. Shigeta, and B. Champagne, J. Chem. Phys. **136**, 024315 (2012).

[24] M. Nakano, R. Kishi, T. Nitta, T. Kubo, K. Nakasuji, K. Kamada, K. Ohta, B. Champagne, E. Botek, and K. Yamaguchi, J. Phys. Chem. A **109**, 885 (2005).

[25] M. Nakano, H. Nagai, H. Fukui, K. Yoneda, R. Kishi, H. Takahashi, A. Shimizu, T. Kubo, K. Kamada, K. Ohta, B. Champagne, and E. Botek, Chem. Phys. Lett. **467**, 120 (2008).

[26] H. Nagai, M. Nakano, K. Yoneda, R. Kishi, H. Takahashi, A. Shimizu, T. Kubo, K. Kamada, K. Ohta, E. Botek, and B. Champagne, Chem. Phys. Lett. **489**, 212 (2010).

[27] K. Kamada, K. Ohta, T. Kubo, A. Shimizu, Y. Morita, K. Nakasuji, R. Kishi, S. Ohta, S.-i. Furukawa, H. Takahashi, and M. Nakano, Angew. Chem., Int. Ed. **46**, 3544 (2007).

[28] H. Kishida, K. Hibino, A. Nakamura, D. Kato, and J. Abe, Thin Solid Films **519**, 1028 (2010).

[29] R. J. Bartlett and G. D. Purvis III, Phys. Rev. A **20**, 1313 (1979).

[30] P. Limacher, L. Qingxu, and H. Lüthi, J. Chem. Phys. **135**, 014111 (2011).

[31] H. Sekino, Y. Maeda, M. Kamiya, and K. Hirao, J. Chem. Phys. **126**, 014107 (2007).

[32] J.-W. Song, M. Watson, H. Sekino, and K. Hirao, J. Chem. Phys. **129**, 024117 (2008).

[33] B. Kirtman, S. Bonness, A. Ramirez-Solis, B. Champagne, H. Matsumoto, and H. Sekino, J. Chem. Phys. **128**, 114108 (2008).

[34] T. Toto, J. Toto, C. de Melo, M. Hasan, and B. Kirtman, Chem. Phys. Lett. **244**, 59 (2009).

[35] J.-W. Song, M. Watson, H. Sekino, and K. Hirao, Int. J. Quantum Chem. **109**, 2012 (2009).

[36] B. Champagne and B. Kirtman, Int. J. Quantum Chem. **109**, 3103 (2009).

[37] P. A. Limacher, K. V. Mikkelsen, and H. P. Luthi, J. Chem. Phys. **130**, 194114 (2009).

[38] H. Sekino and R. J. Bartlett, J. Chem. Phys. **98**, 3022 (1993).

[39] D. R. Hartree, Proc. Cambridge Philos. Soc. **24**, 89 (1928).

[40] V. Fock, Z. Phys. **61**, 126 (1930).

[41] P. Hohenberg and W. Kohn, Phys. Rev. **136**, B864 (1964).

[42] W. Kohn and L. Sham, Phys. Rev. **140**, A1133 (1965).

[43] B. Champagne, E. A. Perpete, S. J. A. van Gisbergen, E.-J. Baerends, J. G. Snijders, C. Soubra-Ghaoui, K. A. Robins, and B. Kirtman, J. Chem. Phys. **109**, 10489 (1998).

[44] S. J. A. van Gisbergen, P. R. T. Schipper, O. V. Gritsenko, E. J. Baerends, J. G. Snijders, B. Champagne, and B. Kirtman, Phys. Rev. Lett. **83**, 694 (1999).

[45] P. Mori-Sanchez, Q. Wu, and W. Yang, J. Chem. Phys. **119**, 11001 (2003).

[46] M. Kamiya, H. Sekino, T. Tsuneda, and K. Hirao, J. Chem. Phys. **122**, 234111 (2005).

[47] B. Champagne and D. Mosley, J. Chem. Phys. **105**, 3592 (1996).

[48] M. Nakano, R. Kishi, S. Ohta, A. Takebe, H. Takahashi, S.-i. Furukawa, T. Kubo, Y. Morita, K. Nakasuji, K. Yamaguchi, K. Kamada, K. Ohta, B. Champagne, and E. Botek, J. Chem. Phys. **125**, 074113 (2006).

[49] M. Nakano, H. Nagao, and K. Yamaguchi, Phys. Rev. A **55**, 1503 (1997).

[50] M. Nakano, A. Takebe, R. Kishi, S. Ohta, M. Nate, T. Kubo, K. Kamada, K. Ohta, B. Champagne, E. Botek, H. Takahashi, S.-i. Furukawa, Y. Morita, and K. Nakasuji, Chem. Phys. Lett. **432**, 473 (2006).

[51] M. Nakano, S. Yamada, S. Kiribayashi, and K. Yamaguchi, Int. J. Quantum Chem. **70**, 269 (1998).

[52] S. Wouters, P. A. Limacher, D. V. Neck, and P. W. Ayers, J. Chem. Phys. **136**, 134110 (2012).

[53] B. Champagne, D. H. Mosley, M. Vračko, and J.-M. André, Phys. Rev. A **52**, 178 (1995).

[54] B. Champagne, D. H. Mosley, M. Vračko, and J.-M. André, Phys. Rev. A **52**, 1039 (1995).

[55] J. L. Toto, T. T. Toto, and C. P. de Melo, Chem. Phys. Lett. **245**, 660 (1995).

[56] Q. Li, L. Chen, Q. Li, and Z. Shuai, Chem. Phys. Lett. **457**, 276 (2008).

[57] J. Čížek, J. Chem. Phys. **45**, 4256 (1966).

[58] J. Čížek, Adv. Chem. Phys. **14**, 35 (1969).

[59] J. Čížek and J. Paldus, Int. J. Quantum Chem. **5**, 359 (1971).

[60] R. J. Barlett and G. D. Purvis III, Int. J. Quantum Chem. **14**, 561 (1978).
[61] R. J. Bartlett, Annu. Rev. Phys. Chem. **32**, 359 (1981).
[62] G. D. Purvis III and R. J. Bartlett, J. Chem. Phys. **76**, 1910 (1982).
[63] M. Urban, J. Noga, S. J. Cole, and R. J. Bartlett, J. Chem. Phys., **83**, 4041 (1985).
[64] K. Raghavachari, G. W. Trucks, J. A. Pople, and M. Head-Gordon, Chem. Phys. Lett. **157**, 479 (1989).
[65] M. J. O. Deegan and P. J. Knowles, Chem. Phys. Lett. **227**, 321 (1994).
[66] H.-J. Werner and P. J. Knowles, J. Chem. Phys. **89**, 5803 (1988).
[67] P. J. Knowles and H.-J. Werner, Chem. Phys. Lett. **145**, 514 (1988).
[68] R. J. Gdanitz and R. Ahlrichs, Chem. Phys. Lett. **143**, 413 (1988).
[69] P. G. Szalay and R. J. Bartlett, Chem. Phys. Lett. **214**, 481 (1993).
[70] H.-J. Werner and P. J. Knowles, Theor. Chem. Acc. **78**, 175 (1991).
[71] J. B. Robinson and P. J. Knowles, J. Chem. Phys. **136**, 054114 (2012).
[72] P. J. Knowles and B. Cooper, J. Chem. Phys. **133**, 224106 (2010).
[73] J. B. Robinson and P. J. Knowles, J. Chem. Phys. **135**, 044113 (2011).
[74] R. J. Bartlett and J. Noga, Chem. Phys. Lett. **150**, 29 (1988).
[75] P.-D. Fan, K. Kowalski, and P. Piecuch, Mol. Phys. **103**, 2191 (2005).
[76] P.-D. Fan and P. Piecuch, Adv. Quantum Chem. **51**, 1 (2006).
[77] P. Piecuch, I. S. O. Pimienta, P.-D. Fan, and K. Kowalski, ACS Symp. Ser. **958**, 37 (2007).
[78] P. Piecuch, K. Kowalski, P.-D. Fan, and I. S. O. Pimienta, Prog. Theor. Chem. Phys. **12**, 119 (2010).
[79] T. Van Voorhis and M. Head-Gordon, J. Chem. Phys. **113**, 8873 (2000).
[80] B. Cooper and P. J. Knowles, J. Chem. Phys. **133**, 234102 (2010).
[81] F. A. Evangelista, J. Chem. Phys. **134**, 224102 (2011).
[82] W. Kutzelnigg, Mol. Phys. **94**, 65 (1998).
[83] W. Kutzelnigg, Theor. Chim. Acta **80**, 349 (1991).
[84] J. Arponen, Ann. Phys. (N.Y.) **151**, 311 (1983).
[85] T. Van Voorhis and M. Head-Gordon, Chem. Phys. Lett. **330**, 585 (2000).
[86] C. Kollmar and A. Heßelmann, Theor. Chem. Acc. **127**, 311 (2009).
[87] J. B. Robinson and P. J. Knowles, Phys. Chem. Chem. Phys. **14**, 6729 (2012).
[88] J. B. Robinson and P. J. Knowles, "Benchmark quasi-variational coupled cluster calculations of multiple bond breaking," J. Chem. Theory Comput. (in press).
[89] A. Einstein, Ann. Phys. **354**, 769 (1916).
[90] K. A. Brueckner, Phys. Rev. **96**, 508 (1954).
[91] R. K. Nesbet, Phys. Rev. **109**, 1632 (1958).
[92] N. C. Handy, J. A. Pople, M. Head-Gordon, K. Raghavachari, and G. W. Trucks, Chem. Phys. Lett. **164**, 185 (1989).
[93] J. Watts, J. Gauss, and R. Bartlett, J. Chem. Phys. **98**, 8718 (1993).
[94] P. Atkins and R. Friedman, *Molecular Quantum Mechanics*, 4th ed. (Oxford University Press, 2007).
[95] H.-J. Werner, P. J. Knowles, G. Knizia, F. R. Manby, M. Schütz *et al.*, MOLPRO, version 2010.2, a package of *ab initio* programs, 2011, see http://www.molpro.net.
[96] H.-J. Werner, P. J. Knowles, G. Knizia, F. R. Manby, and M. Schütz, WIREs Comput. Mol. Sci. **2**, 242 (2012).
[97] T. H. Dunning, Jr., J. Chem. Phys. **90**, 1007 (1989).
[98] R. A. Kendall, T. H. Dunning, Jr., and R. J. Harrison, J. Chem. Phys. **96**, 6796 (1992).
[99] G. Bendazzoli, S. Evangelisti, and A. Monari, Int. J. Quantum Chem. **111**, 3416 (2011).
[100] A. Szabo and N. Ostlund, *Modern Quantum Chemistry: Introduction to Advanced Electronic Structure Theory* (Dover, 1996).
[101] R. H. Nobes, J. A. Pople, L. Radom, N. C. Handy, and P. J. Knowles, Chem. Phys. Lett. **138**, 481 (1987).
[102] P. J. Knowles and N. C. Handy, J. Phys. Chem. **92**, 3097 (1988).